The Locations of Satellite Galaxies in a ΛCDM Universe

Ingolfur Agustsson & Tereasa G. Brainerd

Boston University, Institute for Astrophysical Research, 725 Commonwealth Ave., Boston, MA 02215

ingolfur@bu.edu, brainerd@bu.edu

ABSTRACT

We compute the locations of satellite galaxies with respect to their hosts using the Λ CDM GIF simulation. If the major axes of the hosts' images are perfectly aligned with the major axes of their projected mass, the satellites are located preferentially close to the hosts' major axes. In this case, the degree of anisotropy in the satellite locations is a good tracer of the flattening of the hosts' halos. If all hosts have luminous circular disks, the symmetry axes of the projected mass and light are not perfectly aligned, and the locations of the satellites depend upon how the hosts' disks are placed within their halos. If the disk angular momentum vectors are aligned with the major axes of the halos, the satellites show a pronounced "Holmberg effect". If the disk angular momentum vectors are aligned with the intermediate axes of the local large scale structure, the distribution of satellite locations is essentially isotropic. If the disk angular momentum vectors are aligned with either the minor axes or with the net angular momentum vectors of the halos, the satellites are distributed anisotropically about their hosts, with a preference for being found nearby the hosts' major axes. This agrees well with the observation that satellite galaxies in the Sloan Digital Sky Survey tend to be found nearby the major axes of their hosts, and suggests that the mass and light of SDSS host galaxies must be fairly well aligned in projection on the sky.

Subject headings: dark matter — galaxies: dwarf — galaxies: fundamental parameters — galaxies: halos — galaxies: structure

1. Introduction

The standard cold dark matter (CDM) scenario predicts that large, bright galaxies reside within mildly–flattened halos that accrete mass preferentially along filaments. Recent work on weak galaxy–galaxy lensing (e.g., Guzik & Seljak 2002; Hoekstra et al. 2004; Kleinheinrich et al. 2004) and the kinematics of satellite galaxies (e.g., Prada et al. 2002; Brainerd 2004) suggests that the spherically–averaged potentials of large field galaxies are in quite good agreement with the predictions of CDM (i.e., the Navarro, Frenk & White, NFW, profile; Navarro, Frenk & White 1995, 1996, 1997). Within the virial radius, r_{200} , the median projected ellipticity of CDM galaxy halos is $\epsilon_{\rm halo} \sim 0.3$. On scales $r << r_{200}$, the effects of gas cooling will make the halos somewhat rounder that this, but on scales $r \sim r_{200}$ the shapes of the halos are not greatly affected by the baryons (e.g., Kazantzidis et al. 2004.) In order to fully test the CDM paradigm one would ideally like to compare this prediction of flattened CDM halos to the observed shapes of the dark halos in our universe. Direct constraints on the actual shapes of dark galaxy halos are, however, much more difficult to obtain than are constraints on the spherically–averaged halo potentials (see, e.g., the review by Sackett 1999).

Hoekstra et al. (2004) found that their galaxy–galaxy lensing signal was consistent with the halos of the lens galaxies being flattened to the degree expected from CDM: $\epsilon_{\text{halo}} = 0.33^{+0.07}_{-0.009}$. This is an exciting result, but is a bit controversial for two reasons. First, structures larger than galaxies (i.e., nearby groups or clusters of galaxies) may contribute an external shear that could affect the inferred flattening of galaxy–mass halos. Second, Hoekstra et al. (2004) made two simplifying assumptions about their lens galaxies: (1) mass and light are perfectly aligned in projection on the sky, and (2) the ellipticities of the dark halos of the lens galaxies are related to the ellipticities of the observed images through a constant multiplicative factor, $\epsilon_{\text{halo}} = f \epsilon_{\text{lens}}$, where ϵ_{lens} is the ellipticity of the light emitted by the lens galaxies.

Here we investigate another possible indicator of the shapes of dark galaxy halos: the location of small, faint satellite galaxies with respect to the symmetry axes of large, bright "host" galaxies. This approach is complimentary to galaxy–galaxy lensing since, in both cases, an ensemble average over many galaxies is necessary to detect a signal. In the case of galaxy–galaxy lensing, the weak lensing shear is too small to be detected convincingly from a single lens galaxy and, hence, thousands of lenses are needed. In the case of the locations of satellite galaxies, standard host–satellite selection algorithms generally yield only one or two satellites per host in the large redshift surveys. Therefore, a convincing measurement of the locations of satellites relative to their hosts requires a large number of objects.

Our study is motivated by a recent finding that the satellites of isolated host galaxies

in the Sloan Digital Sky Survey are distributed anisotropically about their hosts (Brainerd 2005). In particular, on scales less than a few hundred kiloparsecs, the SDSS satellites are located preferentially close to the major axes of their hosts. This is the exact opposite of the so-called "Holmberg effect" (e.g., Holmberg 1969; Lynden-Bell 1982; Majewski 1994; Zartisky et al. 1997), in which satellite galaxies are found preferentially close to the minor axes of their hosts. It could be argued that the disagreement between these early studies and that of Brainerd (2005) is merely the result of small number statistics in the early samples of hosts and satellites. However, Sales & Lambas (2004) analyzed the location angles of satellite galaxies in the Two Degree Field Galaxy Redshift Survey and, using a sample size similar to that of Brainerd (2005), Sales & Lambas (2004) concluded that the majority of the 2dFGRS satellites were distributed isotropically about their hosts. In a very small, restricted subsample of their data, however, Sales & Lambas (2004) found weak evidence for the 2dFGRS satellites to be located preferentially close to the minor axes of the hosts (i.e., evidence for the Holmberg effect).

This disagreement between Brainerd (2005) and Sales & Lambas (2004) has fueled controversy over whether or not satellite galaxies have a preferred location relative to their hosts. A recent reanalysis of the 2dFGRS data by Sales & Lambas has, however, revealed an error in the host position angles in the original data and when the error is corrected the satellites of the 2dFGRS hosts show the same anisotropy that was found by Brainerd (2005): a preference for clustering near the major axes of the host galaxies (Sales & Lambas 2006, in preparation).

On the theoretical side, previous numerical work leads us to expect that satellite galaxies in CDM universes will not be spherically—distributed around their host galaxies. Knebe et al. (2004) found that the orbits of satellites of primary galaxies in cluster environments were located preferentially within a cone of opening angle 40°. The structure of CDM halos is largely independent of the halo mass scale (e.g., Moore et al. 1999), so this suggests that the satellites of isolated host galaxies in CDM models ought to be roughly aligned with the major axes of the host halos. Further, recent numerical work by Libeskind et al. (2005) and Zentner et al. (2005) on the luminous satellites of Milky Way—type halos has shown that the satellites tend to lie in highly—flattened structures that are essentially embedded in the principle planes of the host halos (i.e., the plane defined by the major and intermediate moments of the inertia tensor). Our study complements these investigations by using a much larger and, hence more statistically significant, sample of objects.

To explore the possibility that the location of satellite galaxies relative to their hosts may serve as a tracer of the dark mass distribution around host galaxies, we use the Λ CDM GIF simulation (Kauffmann et al. 1999) to pose the following questions:

- Are satellite galaxies in a ΛCDM universe distributed isotropically or anisotropically about their hosts?
- How does the distribution of satellites compare to the distribution of dark mass surrounding the hosts?
- If the light emitted by the hosts comes from a disk, how does the orientation of the disk within the host's halo affect the inferred satellite distribution?

Throughout, we analyze the simulation in the same way in which an observer would analyze a combined imaging and redshift survey. That is, we work in terms of the locations of objects and the shapes of halos as seen in projection on the sky, and we select host and satellite galaxies from the simulation using the same types of algorithms that are used to select hosts and satellites from observational data.

The outline of the paper is as follows. In §2 we discuss the GIF simulation and the way in which host galaxies and their satellites are selected. In §3 we make a simple assumption that the mass and light of host galaxies are perfectly aligned in projection on the sky and we compute the location angles of the satellite galaxies with respect to the major axes of the projected host halos. In §4 we model the luminous regions of the host galaxies as circular disks and we embed the disks within the halos according to various prescriptions. We then compute the location angles of the satellite galaxies with respect to the major axes of the projected host disks. A summary and discussion of our results is given in §5.

2. Hosts and Satellites in the ΛCDM GIF Simulation

The GIF simulations are a suite of CDM simulations which combine adaptive P³M N-body techniques with semi-analytic galaxy formation. The inclusion of semi-analytic galaxy formation eliminates the "overmerging problem" in which galaxies within halos that merge to form larger structures (i.e., groups and clusters) quickly lose their identities as individual objects. The location of a luminous galaxy in the GIF simulations is initially identified with the most bound particle in a given halo. When two or more halos merge, the luminous galaxies within the halos maintain their separate identities with the exception that the luminous galaxies may ultimately merge on a time scale that is set by dynamical friction. It is these luminous galaxies whose locations are associated with individual particles that we use to identify hosts and satellites within the simulation and, hence, the satellite population which we investigate does not suffer from an artificial overmerging problem. For a complete discussion of the way in which luminous galaxies are allowed to merge in the GIF simulations, see §4.4 and §4.8 of Kauffmann et al. (1999).

Since it seems that our universe is consistent with having cosmological parameters of $\Omega_{m0} = 0.3$, $\Lambda_0 = 0.7$, and $H_0 = 70 \text{ km s}^{-1} \text{ Mpc}^{-1}$, we use only the ΛCDM GIF simulation for our analysis. The ΛCDM GIF simulation has these particular cosmological parameters, a co-moving box size of 201.7 Mpc, a mass per particle of $2 \times 10^{10} M_{\odot}$, and a softening length of 28.6 kpc. The simulation can be downloaded from the GIF project website, http://www.mpa-garching.mpg.de/GIF, for a wide range of redshifts. Here we use primarily the present-epoch data since the large redshift surveys (i.e., SDSS and 2dFGRS) that have been used to investigate the observed location of satellite galaxies relative to their hosts are restricted to fairly low redshift.

We specifically use the z=0 Λ CDM GIF galaxy catalog in which the magnitudes of the galaxies are given in the SDSS band passes (i.e., the file called galsl_sdss.cat_1178). In addition, we use the dark matter particle file called compd4001.1178. The luminous galaxies in the simulation have known properties such as stellar mass, luminosity, and color, as well as known locations and peculiar velocities. Dark matter halos which surround the luminous galaxies must necessarily be identified from the mass particles via a halo finding routine. A file called halos.propl_1178 that contains dark halo information is provided by the GIF group, but we choose not to use this file. The information in halos.propl_1178 is based upon halos that were found using a friends-of-friends algorithm, which is known to often link into one single object two or more nearby halos that have distinct, identifiable centers. Instead of friends-of-friends halos, then, we simply use the particle file compd4001.1178 to define dark matter halos as the mass contained within spheres of radius r_{200} , where r_{200} is the radius inside which the mean interior mass density is equal to 200 times the critical mass density. This definition of the virial radius and virial mass is consistent with the formalism adopted by Navarro, Frenk & White (1995, 1996, 1997).

For our analysis, we require the dark matter halos of the host galaxies to have a sufficiently large number of particles for a reasonable measurement of the halo shape to be made. Therefore, we restrict our analysis to host galaxies with dark matter halos that contain 100 or more particles within r_{200} (i.e., the minimum halo mass for our host galaxies is $2 \times 10^{12} M_{\odot}$). We make no such minimum mass restriction on the satellite galaxies. The virial radii and the centers of the host galaxy halos are computed in 3 dimensions using a standard iterative scheme. The halo is initially assumed to be centered on the location of the luminous galaxy. The virial radius is then defined to be the radius of a sphere of particles, centered on the luminous galaxy, for which the mean interior mass density is equal to 200 times the critical density. The center of mass of the initial sphere of particles is computed, and this is then used to define a new center from which a new sphere of particles is obtained and yet another center of mass is computed. The process is repeated until convergence is reached. Convergence occurs within only a few iterations and, in projection on the sky, the

location of the particle that represents the position of the luminous galaxy is typically offset by less than half a smoothing length from center of mass of the galaxy's halo.

Host-satellite systems are selected by rotating the simulation randomly and then projecting the simulation along the line of sight. The resulting line of sight velocities, coordinates on the "sky", and the apparent magnitudes of the GIF galaxies are then used as direct substitutes for the type of data that would be available in a large redshift survey. Results below are obtained from 100 random rotations of the simulation. Following Brainerd (2005), three different methods are used to select isolated hosts and their satellites via a combination of line of sight velocity difference, |dv|, projected radius from the host, r_p , and apparent magnitude difference, $\Delta m \equiv m_1 - m_2$, where $m_1 > m_2$. Throughout we take the coordinates and peculiar velocities of the GIF galaxies to be those of the individual particles that flag the presence of a luminous galaxy in the simulation. In Sample 1, the apparent magnitude difference between a host galaxy and any other galaxy that lies within $r_p < 700 \text{ kpc}$ and $|dv| < 1000 \text{ km s}^{-1}$ must be $\Delta m \ge 1.0$. Satellites of Sample 1 hosts must fall within $r_p < 500~{\rm kpc}$ and $|dv| < 500~{\rm km~s^{-1}}$ and have $\Delta m \geq 2.0$. In Sample 2, the apparent magnitude difference between a host galaxy and any other galaxy that lies within $r_p < 2.86 \text{ Mpc}$ and $|dv| < 1000 \text{ km s}^{-1} \text{ must be } \Delta m \geq 0.75$. Satellites of Sample 2 hosts must lie within $r_p < 500$ kpc and |dv| < 1000 km s⁻¹ and have $\Delta m \geq 1.5$. In Sample 3, the magnitude difference between a host galaxy and any other galaxy that lies within $r_p < 500 \ \mathrm{kpc}$ and $|dv| < 1000 \ \mathrm{km \ s^{-1}}$ must be $\Delta m \geq 2.25$. Further, the magnitude difference between a host galaxy in Sample 3 and any other galaxy that lies within $r_p < 1~{\rm Mpc}$ and $|dv| < 1000 \text{ km s}^{-1} \text{ must be } \Delta m \geq 0.75$. Satellites of Sample 3 hosts must lie within $r_n < 500 \text{ kpc}$ and $|dv| < 500 \text{ km s}^{-1}$, and have $\Delta m \geq 2.25$. These criteria select only very isolated hosts and their satellites, and it is worth noting that both the Milky Way and M31 would be rejected as host galaxies under these restrictions.

In order to eliminate a small number of systems that pass the above tests but which are, in reality, more likely to be representative of cluster environments rather than isolated host–satellite systems, we impose two further restrictions: (1) the sum total of the luminosities of the satellites of a given host must be less than the luminosity of the host, and (2) the total number of satellites of a given host must be less than 9. In addition, we restrict our analysis to hosts with luminosities in the range $0.5L_{bJ}^* \leq L \leq 5.5L_{bJ}^*$ since Brainerd (2004) found that outside this luminosity range the kinematics of the satellites in the Λ CDM GIF simulation were not consistent with a virialized population. This last criterion eliminates only a small number of possible hosts from the analysis ($\sim 2\%$ of the Sample 1 hosts, $\sim 7\%$ of the Sample 2 hosts, and $\sim 3\%$ of the Sample 3 hosts). To compute the b_J magnitudes of the GIF galaxies, the SDSS magnitudes given in the file galsl_sdss.cat_1178 were converted

using the photometric transformation of Norberg et al. (2002):

$$b_J = g' + 0.155 + 0.152(g' - r'). (1)$$

For the cosmological parameters used in the Λ CDM GIF simulation, the absolute magnitude of an L^* galaxy in the b_J band is $M_{b_J}^* = -20.43 \pm 0.07$.

After all of the above selection criteria have been imposed, we find that on average the individual rotations of the simulation yield 1786 hosts and 5752 satellites in Sample 1, 317 hosts and 1208 satellites in Sample 2, and 949 hosts and 2865 satellites in Sample 3.

A final important point is that, while the host galaxies in the GIF simulation have known luminosities, there are no actual *images* of the galaxies in the simulation. For our investigation, then, we need to *define* an image for each of the host galaxies in order to determine the locations of the satellites with respect to the symmetry axes of the host images. In all cases, we define the images of the host galaxies to be ellipses on the sky; however, the orientations of the image ellipses are obtained in a number of different ways. To begin, we assume that the mass and the light of the host galaxies are perfectly aligned in projection on the sky. In this case, the major axis of the image of the host galaxy corresponds to the major axis of the projected halo mass distribution. Next, we assume that all host galaxies are circular disks and we embed the disks within the hosts' halos using various prescriptions. In these cases, the major axis of the image of a host galaxy is the major axis of the host's circular disk as seen in projection on the sky, and here the major axis of the light is not necessarily aligned with a symmetry axis of the projected halo mass. We will justify our various choices for the host images in the sections below.

3. Alignment of Light and Mass in the Hosts

In this section we make a very simple assumption that the major axis of the image of a host galaxy is perfectly aligned with the major axis of the projected mass distribution of its halo. This assumption can be partially justified by the argument that galaxies are relaxed systems and, if the dark matter halos are substantially flattened, then the most dynamically reasonable expectation is that mass and light should be fairly well aligned. Direct determinations of the degree of alignment of mass and light in observed galaxies are difficult and rare, but in a study of strong lens galaxies Keeton et al. (1998) found that the major axes of the mass and light in the lens galaxies were aligned to within 10° in projection on the sky.

To begin our analysis of the locations of satellite galaxies with respect to their hosts, we use the mass contained within the spherical overdensity region of radius r_{200} around each

host to compute the principle moments of inertia of the halo and, thus, the halo's equivalent ellipsoid. This yields axis ratios b/a and c/a for each of the halos, where we define $a \ge b \ge c$. A triaxiality parameter is then computed for each of the host halos:

$$T = \frac{a^2 - b^2}{a^2 - c^2}. (2)$$

Here T=0 indicates a purely oblate object and T=1 indicates a purely prolate object. To define the major axis of a host galaxy, we project the 3-dimensional ellipsoid of its halo onto the sky. This yields an ellipse with semi-major axis α , semi-minor axis β , and ellipticity $\epsilon_{\text{halo}} = 1 - \beta/\alpha$. The major axis of the light emitted by the host galaxy is then defined to be the major axis of the halo's projected ellipsoid and this is used as the symmetry axis relative to which the location angles of the satellite galaxies are measured.

Figure 1 shows the distribution of host luminosities, the mass function of the host halos, the distribution of the host halo triaxiality parameters, the distribution of the number of satellites per host, the distribution of apparent magnitude differences between the hosts and their satellites, and the distribution of the ratio of stellar masses of the satellites and hosts. The median host luminosity is $1.5L_{b_J}^*$, $1.9L_{b_J}^*$ and $1.8L_{b_J}^*$ for Samples 1, 2 and 3, respectively. The median virial mass of the host halos is $3.5 \times 10^{12} M_{\odot}$, $4.1 \times 10^{12} M_{\odot}$ and $3.5 \times 10^{12} M_{\odot}$ for Samples 1, 2 and 3, respectively, and the median host halo triaxiality is T=0.6 for all three host–satellite samples. The bottom panels of Figure 1 show that our algorithm for finding hosts and satellites clearly selects satellites that are considerably smaller and fainter than their hosts.

Since the host halos are not resolved particularly well (i.e., they contain of order hundreds of particles, not thousands), for the remainder of this particular section we restrict our analysis to systems for which the projected ellipsoid of the host's halo has ellipticity $\epsilon_{\text{halo}} > 0.2$. This insures that the orientation of the major axis of the host is well–determined. When this ellipticity requirement is imposed, the different rotations of the simulation yield an average of 1793 hosts and 5769 satellites in Sample 1, 320 hosts and 1209 satellites in Sample 2, and 957 hosts and 2892 satellites in Sample 3.

For each of the host–satellite samples, we compute the location angles of the satellites relative to the major axes of the hosts. These are simply polar angles, ϕ , on the sky where $\phi = 0^{\circ}$ corresponds to a satellite that is located along the direction of the host's major axis and $\phi = 90^{\circ}$ corresponds to a satellite that is located along the direction of the host's minor axis. Shown Figure 2 are the differential probability distributions, $P(\phi)$, and the cumulative probability distributions, $P(\phi \le \phi_{\text{max}})$, for the location angles of the satellites measured with respect to the major axes of their hosts. Here the null hypothesis to which $P(\phi)$ and $P(\phi \le \phi_{\text{max}})$ should be compared is that the satellite galaxies are distributed spherically

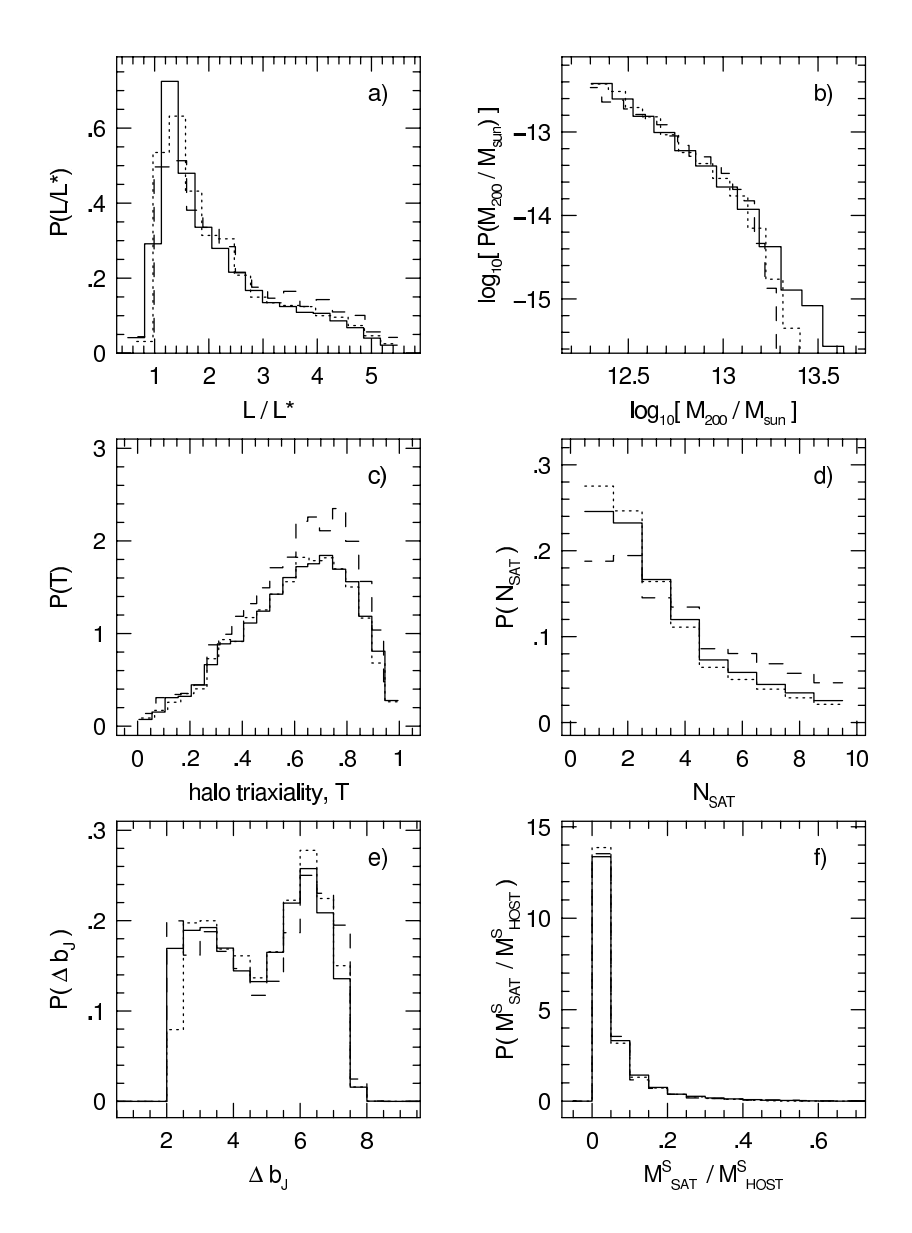


Fig. 1.— a) Probability distribution of host luminosities, b) Host halo mass function, c) Probability distribution of host halo triaxialities, d) Probability distribution for the number of satellites per host, e) Probability distribution for apparent magnitude differences between hosts and satellites, $\Delta b_J \equiv b_J^{\rm sat} - b_J^{\rm host}$, f) Probability distribution for the ratio of satellite stellar mass to host stellar mass. In all panels the different line types correspond to the different host–satellite samples: Sample 1 (solid), Sample 2 (dashed), Sample 3 (dotted). See text for host and satellite selection criteria.

about their hosts. This would give rise to a circularly–symmetric distribution of satellites on the sky. A rotation of a spherically–symmetric distribution through any combination of Euler angles always gives rise to a 2–d distribution that is circularly–symmetric. Hence, any deviation in the satellite distribution from pure circular symmetry cannot be caused simply by projection and/or rotation effects and must reflect an underlying non–spherical 3–d distribution of the satellites.

The left panels of Figure 2 show $P(\phi)$ for the GIF satellites, from which it is clear that they show a strong preference for alignment with the major axes of the projected halo mass. The degree of anisotropy in the satellite location angles is nearly identical for all three host-satellite samples. The right panels of Figure 2 show $P(\phi \leq \phi_{\text{max}})$ for the location angles of the satellites (solid lines), as well as $P(\phi \leq \phi_{\text{max}})$ for the location angles of the mass particles that are contained within the host halos (dashed lines). From the right panel of Figure 2, then, the distribution of satellite galaxies relative to the major axes of their hosts is very similar to the distribution of the mass particles in the projected halos. The satellites show a slightly flatter distribution than the mass particles, but overall the satellites trace the projected shapes of the halos rather well. We demonstrate this further in the top panel of Figure 3, where we show the median location angle of the satellites and the mass particles as a function of the ellipticity of the projected halo. The median location angles decrease approximately linearly with halo ellipticity, although the slope is a bit steeper for the satellites than it is for the mass particles. The relationship is especially linear for $0.2 < \epsilon_{\rm halo} < 0.35$, yielding slopes of $-57^{\circ} \pm 2^{\circ}$ for the satellites and $-49^{\circ} \pm 0.9^{\circ}$ for the mass particles.

Brainerd (2005) found that the anisotropy of the location angles of SDSS satellite galaxies was most pronounced on small scales ($r_p \lesssim 100 \; \mathrm{kpc}$) and that satellites with $r_p \gtrsim 100 \; \mathrm{kpc}$ were distributed rather isotropically. Brainerd (2005) speculated that this could indicate that the virial region of the host halos extended to only about 100 kpc, with satellites at larger radii being part of an infalling population. We investigate this possibility in the bottom panel of Figure 3, where we show the median satellite location angle as a function of the satellite's projected radius, scaled by the virial radius of the halo (i.e., r_p/r_{200}). From this figure, then, the anisotropy in the satellite location angles is present over all scales, but it appears to be most pronounced for satellites with $r_p \sim r_{200}$. In addition, the anisotropy persists to projected radii of order $2r_{200}$. This result compares rather poorly to the observation that the satellites of SDSS hosts seem to be distributed isotropically on large scales, and the resolution of this discrepancy is not immediately obvious.

Finally, to allay any lingering concerns that overmerging of the satellite population could affect the distribution of the location angles of the GIF satellites, we compute $P(\phi)$

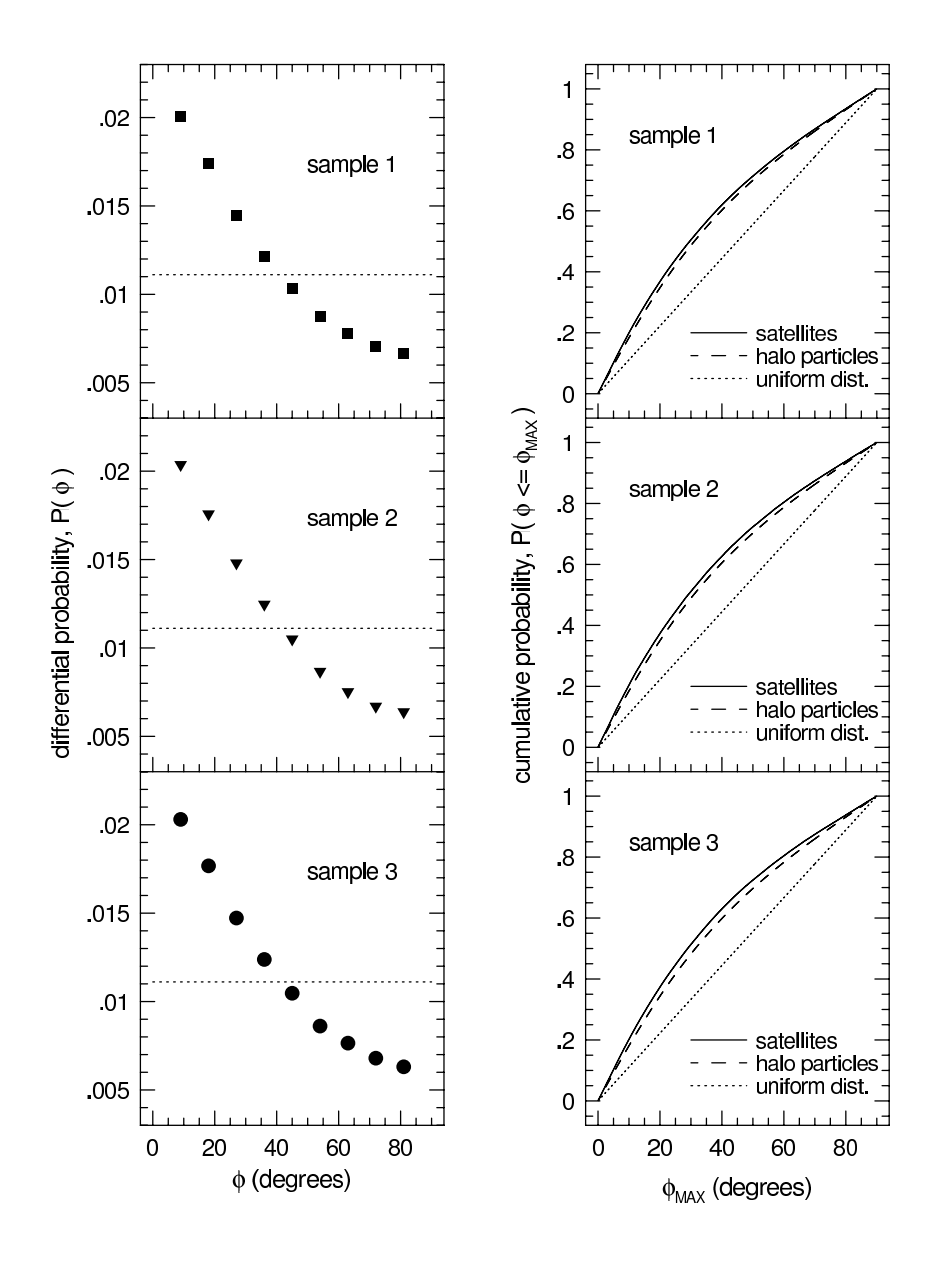


Fig. 2.— Left panels: Differential probability distribution function for the location angles of the satellites, measured with respect to the major axes of the projected halo mass. Here $\phi = 0^{\circ}$ corresponds to alignment with the projected halo major axis and $\phi = 90^{\circ}$ corresponds to alignment with the projected halo minor axis. Dotted line shows the expectation for a uniform (circularly–symmetric) distribution of satellites. Right panels: Cumulative probability distribution for the location angles of the satellites (solid lines) and halo mass particles (dashed lines) with respect to the major axes of the projected halo mass. Top panels: Sample 1. Middle panels: Sample 2. Bottom panels: Sample 3. All satellites located within a projected radius of $r_p < 500$ kpc have been used in the calculations.

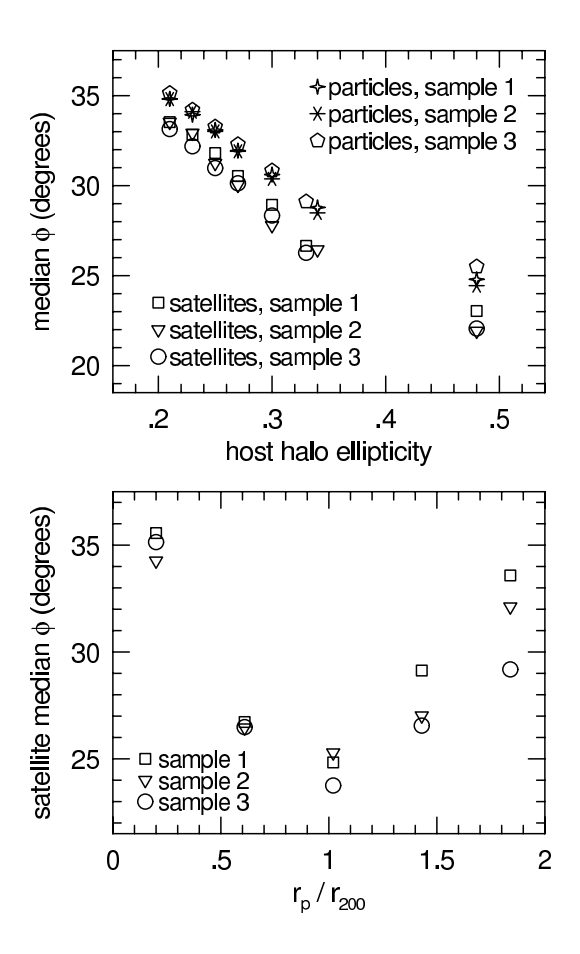


Fig. 3.— Top panel: Median location angles of satellites and halo particles as a function of the ellipticity of the projected halo. All satellites with $r_p < 500$ kpc and all particles within r_{200} have been used in the calculation. Bottom panel: Median location angles of satellites as a function of projected radius on the sky, scaled by the virial radius of the host halo. The median host halo virial radius is ~ 275 kpc in all three samples. Bins have been chosen such that an equal number of objects falls within each bin.

and $P(\phi \le \phi_{\text{max}})$ for satellites that are present at z=0 but which are known to have been in existence since at least z=0.52. That is, we restrict our analysis to satellites in the file galsl_sdss.cat_1178 that can also be found in the file galsl_sdss.cat_0671, the z=0.52 galaxy catalog in which magnitudes are given in the SDSS band passes. (Note that z=0.52 is the highest redshift for which galaxy magnitudes are available in the SDSS band passes.) Roughly 60% of the satellites that are present at z=0 can be traced back to z=0.52 as unique objects. Shown in Figure 4 are $P(\phi)$ and $P(\phi \le \phi_{\text{max}})$ for these satellites that are known to be "old" (filled points and dotted lines, respectively) compared to $P(\phi)$ and $P(\phi \le \phi_{\text{max}})$ for all satellites at z=0 (open points and dashed lines, respectively). The probability distributions at z=0 for the "old" satellites are statistically identical to the probability distributions for all satellites at z=0, and we therefore conclude that the anisotropy in the satellite location angles at z=0 is independent of the ages of the satellites and is not strongly affected by overmerging in the simulation.

4. Misalignment of Light and Mass in the Hosts?

The sense of the anisotropy that was found in the previous section is in excellent agreement with the sense of the anisotropy shown by the SDSS satellites (i.e., a preference for location nearby the major axes of the host galaxies). However, the *size* of the effect is grossly different. The median location angle for the GIF satellites in the previous section is $\phi_{\rm med}^{\rm GIF} \sim 29^{\circ}$, while for the SDSS satellites the median location angle is $\phi_{\rm med}^{\rm SDSS} \sim 40.5^{\circ}$ (e.g., Brainerd 2005). In other words, if the major axes of the light emitted by the GIF hosts were perfectly aligned with the major axes of their projected halos, our results in §3 predict that the distribution of satellites about their host galaxies should be much more anisotropic than is observed in our universe.

There are at least two possible explanations for this. First, in the previous section we focused on halos with projected ellipticities of $\epsilon_{\rm halo} > 0.2$. This necessarily biases the sample of satellite galaxies in the simulation compared to observed galaxies in the universe. That is, since one cannot see the dark matter halos of host galaxies in the real universe, one cannot reject the satellites of host galaxies whose halos happen to be rather round in projection. We know from the numerical work of Libeskind et al. (2005) and Zentner et al. (2005) that in CDM universes the luminous satellites of Milky Way–type halos tend to lie in highly–flattened structures that are embedded in the principle planes of the host halos. This is a natural consequence of the infall of mass and galaxies along filaments. Thus, by choosing to use only host halos with substantial projected ellipticities in the previous section, we have introduced a bias that optimizes the degree to which the satellite distribution is observed to

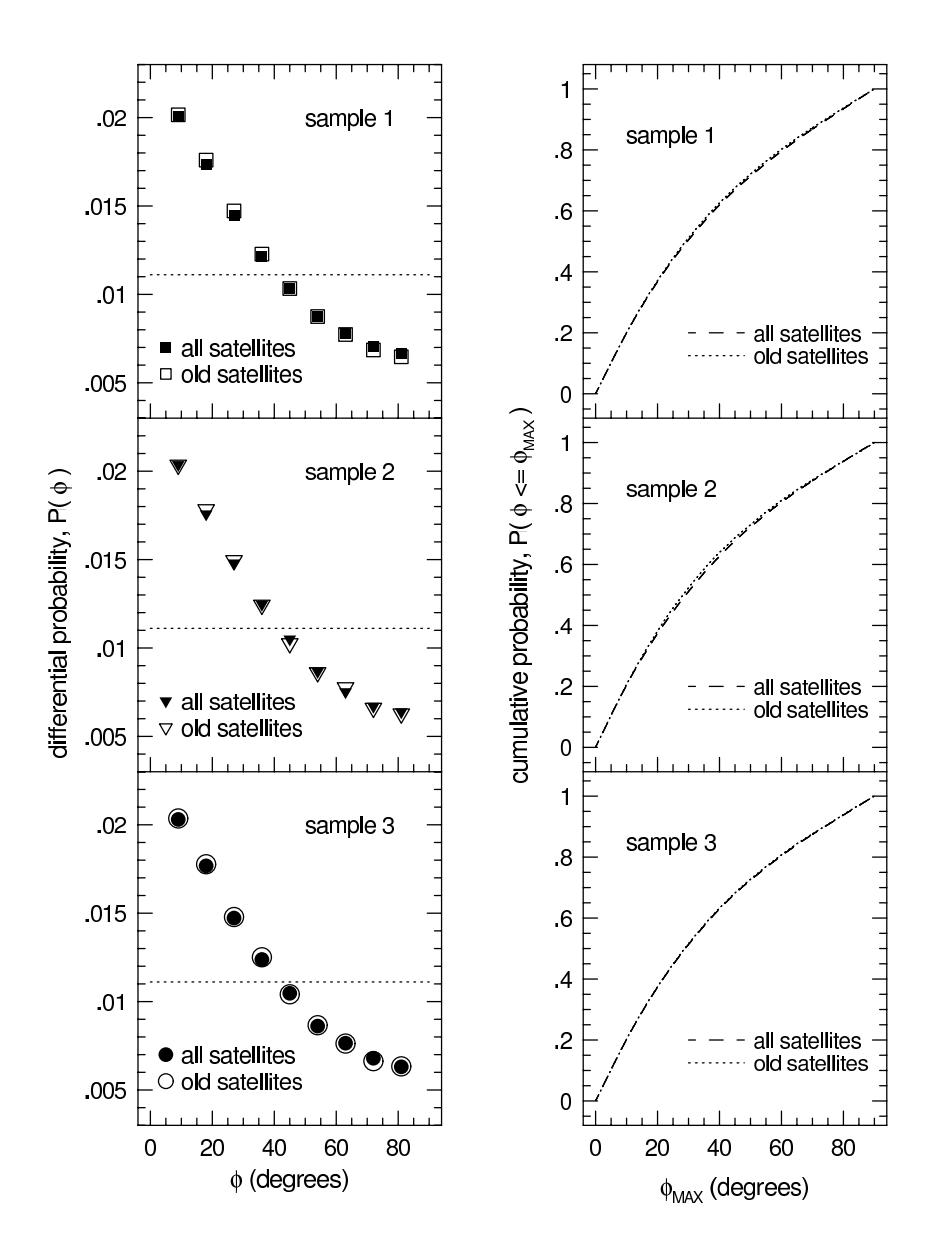


Fig. 4.— Left panels: Differential probability distributions for the location angles of satellites at z=0. Open points show the results for all satellites, filled points show the results for satellites that have existed as unique objects since at least z=0.52. Right panels: Cumulative probability distributions for the location angles of satellites at z=0. Dashed lines show the results for all satellites, dotted lines show the results for satellites that have existed as unique objects since at least z=0.52.

be flattened.

Further, if our previous assumption of perfect alignment of mass and light in the hosts is incorrect, this would contribute to the excessive anisotropy shown by the GIF satellites. We will investigate this possibility in this section by creating artificial structures to represent the luminous regions of the host galaxies. These artificial structures will be embedded within the hosts' halos using a number of different prescriptions, and the location angles of the satellite galaxies will then be computed relative to the major axes of the images that result from projecting the artificial structures onto the sky.

We have visually inspected the images of the 200 brightest SDSS host galaxies in each of Samples 1, 2, and 3 from Brainerd (2005) and we find that 95% of these objects are disk galaxies. This is unsurprising since the host–satellite selection algorithm yields only the very most isolated host galaxies, and large ellipticals are known to be quite rare in low density environments. Also, although there are no images of the GIF hosts in the simulation, we can make a rough assessment of whether the GIF hosts are more likely to be late–type or early–type galaxies based upon their B-band disk-to-bulge ratios. That is, early-type galaxies are expected to have $M(B)_{\text{bulge}} - M(B)_{\text{total}} < 1 \text{ mag. (e.g., Simien \& de Vaucouleurs 1986)}$. B-band bulge luminosities are not provided for the GIF hosts and, therefore, we use the photometric transformation given by Smith et al. (2002) to assign B-band magnitudes:

$$B = g' + 0.47(g' - r') + 0.17$$

and compute $M(B)_{\text{bulge}} - M(B)_{\text{total}}$ for the GIF hosts. Unfortunately, bulge magnitudes are not reported for 35% of our GIF hosts. Of those hosts for which bulge magnitudes are reported, however, only 13% are consistent with being early-type galaxies. Given the observed morphologies of the SDSS hosts and the relative strengths of the bulges of the GIF hosts, then, it seems reasonable to adopt a circular disk as the artificial structure that will represent the luminous regions of the GIF hosts in this section.

In order to place the artificial circular disks within the host halos, we adopt four different methods for defining the orientations of the disk angular momentum vectors, \vec{J} : (1) \vec{J} is aligned with the minor (i.e., "c") axis of the halo's virial mass, (2) \vec{J} is aligned with major (i.e., "a") axis of the halo's virial mass, (3) \vec{J} is aligned with the net angular momentum vector of the halo's virial mass, and (4) \vec{J} is aligned with the intermediate (i.e., "b") axis of the mass that is contained within a radius of 2.5 Mpc, centered on the host. In the first case we are making the naïve assumption that the disk lies in the principle plane of the halo. In the second case, we are assuming that the disk lies perpendicular to the halo's major axis. This choice is the most sought after solution for the Holmberg effect, despite the seemly unnatural orientation of the disk relative to the halo (e.g., Libeskind et al. 2005; Zentner et al. 2005). In the third case we are simply assuming that the angular momentum vectors of

the luminous and dark material are aligned. Our fourth choice for the orientation of the host disks is motivated by work by Navarro, Abadi & Steinmetz (2004) that showed the angular momentum vectors of disk galaxies in CDM universes tend to align with the intermediate axes of the inertia tensor of the local large–scale structure at turnaround. Here we use the inertia tensor of the local large–scale structure at the present epoch but, as Navarro, Abadi & Steinmetz (2004) note, the orientations of the principle axes of the inertia tensor do not change substantially between turnaround and the present. Throughout, we refer to our four methods of placing the disks in the host halos as $\vec{J_c}$, $\vec{J_a}$, $\vec{J_{ang}}$, and $\vec{J_{lss}}$ respectively.

In order to insure that the major axes of the images of host galaxies are well–defined in observational data sets, analyses of the location angles of satellite galaxies with respect to the host major axes are generally restricted to hosts whose images are clearly non–circular (e.g., Sales & Lambas 2004; Brainerd 2005). Following these observational studies, then, we restrict our analysis below to those hosts whose disks have ellipticities $\epsilon_{\rm disk} > 0.2$ in projection on the sky. We use host–satellite selection criteria identical to those in §2, and in Table 1 we list the mean number of hosts and satellites in a given rotation of the simulation. Note that the luminosity distributions, mass functions, distribution of the number of satellites per host, distribution of apparent magnitude differences, and distribution of stellar mass ratios (e.g., Figure 1) are not affected by the increased number of hosts and satellites compared to §3.

In this section, the major axis of a host galaxy's virial mass is not guaranteed to be aligned with the major axis of the host's projected circular disk. In §3 we simply assumed that the offset, $\Delta\theta$, between the major axis of the virial mass of the host galaxy and the major axis of its image would be zero. Shown in the left panels of Figure 5, however, are the actual probability distributions, $P(\Delta\theta)$, that we obtain when we place circular disks within the halos. The form of $P(\Delta\theta)$ is essentially unaffected by the way in which the hosts and satellites are selected (e.g., Samples 1, 2, or 3 for a given choice of disk orientation). However, $P(\Delta\theta)$ is strongly affected by our choice of the orientation of disk angular momentum vectors. In the case of the $\vec{J_c}$ hosts, the light is fairly well aligned with the virial mass in projection on the sky. The median value of $\Delta\theta$ is 6° and only one third of the hosts have values of $\Delta\theta$ that exceed 11°. For the J_a hosts, the light is essentially perpendicular to the virial mass. Here the median value of $\Delta\theta$ is 87° and only one third of the hosts have values of $\Delta\theta$ less than 84.5°. For the $J_{\rm ang}$ hosts, the light is somewhat aligned with the virial mass, the median value of $\Delta\theta$ is $\sim 32^{\circ}$ and one third of the hosts have values of $\Delta\theta$ that exceed $\sim 48^{\circ}$. For the J_{lss} hosts, the orientation of the light is almost completely unrelated to the orientation of the virial mass; the median value of $\Delta\theta$ is $\sim 41^{\circ}$, with one third of the hosts having a value of $\Delta\theta$ that exceeds $\sim 56^{\circ}$.

Table 1: Mean Number of Hosts and Satellites

| Sample | $N_{ m hosts}$ | $N_{\rm sats}$ |
|-------------------------------|----------------|----------------|
| Sample 1, $\vec{J_c}$ | 2828 | 9417 |
| Sample 2, \vec{J}_c | 480 | 1889 |
| Sample 3, \vec{J}_c | 1510 | 4786 |
| Sample 1, \vec{J}_a | 2934 | 9725 |
| Sample 2, \vec{J}_a | 528 | 2064 |
| Sample 3, \vec{J}_a | 1607 | 5065 |
| Sample 1, \vec{J}_{ang} | 2471 | 5809 |
| Sample 2, \vec{J}_{ang} | 443 | 1164 |
| Sample 3, \vec{J}_{ang} | 1345 | 3109 |
| Sample 1, \vec{J}_{lss} | 2864 | 9522 |
| Sample 2, $\vec{J}_{\rm lss}$ | 516 | 2021 |
| Sample 3, \vec{J}_{lss} | 1558 | 4905 |

Shown in the right panels of Figure 5 are the median values of the projected ellipticities of the host halos, $\epsilon_{\rm halo}$, as a function of the ellipticities of the projected circular disks, $\epsilon_{\rm disk}$. Overall, there is a very weak dependence of the median value of $\epsilon_{\rm halo}$ on $\epsilon_{\rm disk}$. In other words, the selection of host galaxies on the basis of a substantial flattening of their *images* is not equivalent to selecting hosts on the basis of a substantial flattening of their *halos*. If, indeed, the locations of the satellites of large host galaxies in our universe are fairly good indicators of the existence of flattened dark matter halos, this suggests that the mean anisotropy of the satellite location angles should be rather insensitive to the mean ellipticity of the host images (i.e., $\langle \phi \rangle$ should be only weakly dependent on $\epsilon_{\rm disk}$). To date, however, measurements of $\langle \phi \rangle$ for satellite galaxies as a function of the ellipticities of their hosts has not been made with the available redshift surveys (i.e., SDSS, 2dFGRS). This is due primarily to the fact that the signal to noise is only barely sufficient to detect the anisotropic distribution of the satellites using the full data set; subdividing the data set into bins of various values of $\epsilon_{\rm disk}$ simply reduces the signal to noise to the point that no conclusive statement can be made about the anisotropy.

In the case of the $\vec{J_c}$ and $\vec{J_a}$ GIF hosts, the median value of $\epsilon_{\rm halo}$ increases with $\epsilon_{\rm disk}$, but the trend is not dramatic. Linear extrapolation of the points in the top right panel of Figure 5 yields median values of $\epsilon_{\rm halo} \sim 0.26$ for edge—on, $\vec{J_c}$ host disks and $\epsilon_{\rm halo} \sim 0.14$ for face—on, $\vec{J_c}$ host disks. Nearly identical results are obtained for the $\vec{J_a}$ hosts. In the case of the $\vec{J}_{\rm ang}$ hosts, the median value of $\epsilon_{\rm halo}$ is essentially independent of $\epsilon_{\rm disk}$. Finally, for the $\vec{J}_{\rm lss}$ hosts the median value of $\epsilon_{\rm halo}$ is a decreasing function of $\epsilon_{\rm disk}$, leading to very slightly

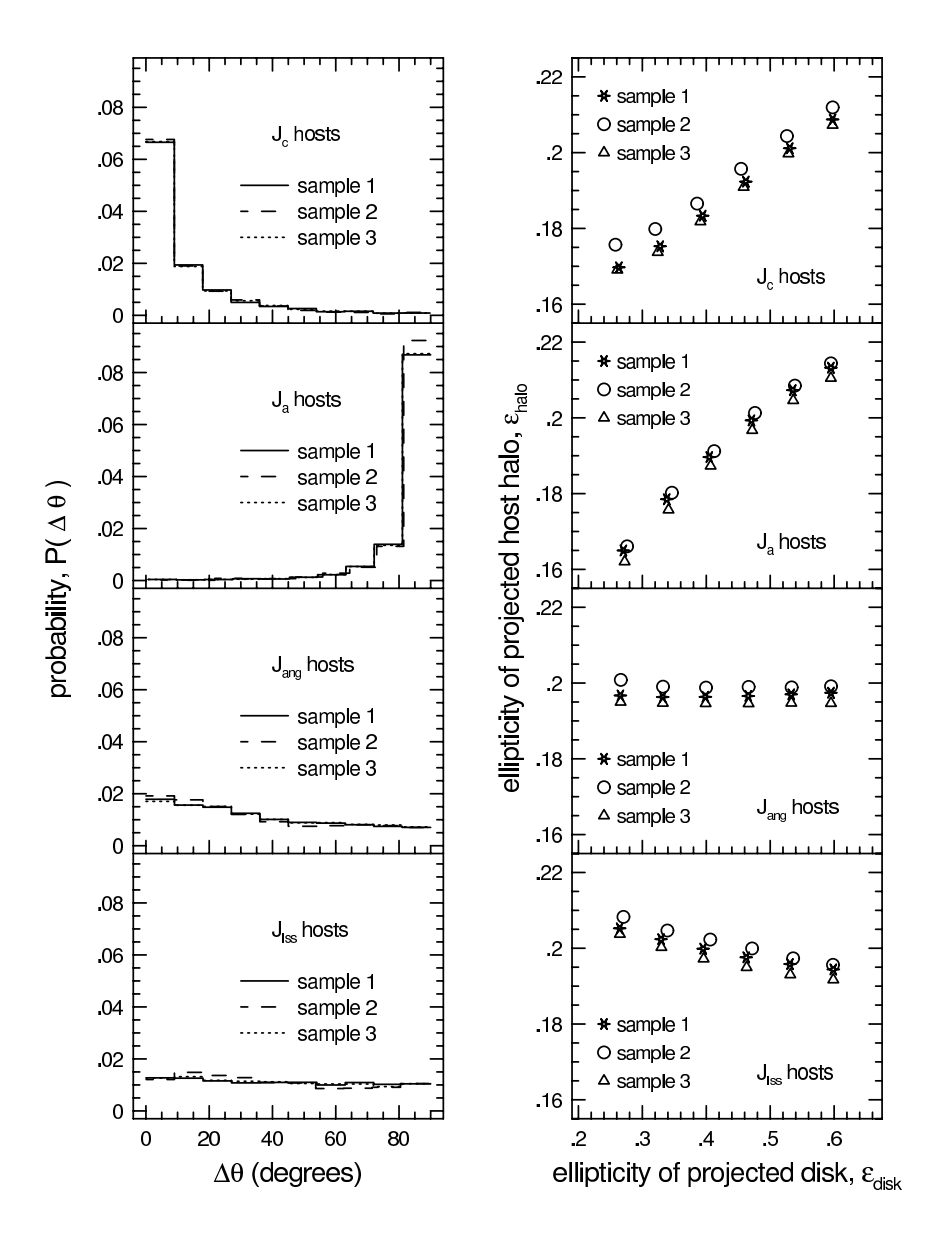


Fig. 5.— Left panels: Probability distribution, $P(\Delta\theta)$, of the offset between the major axis of a host galaxy's projected halo mass and the major axis of the host's projected circular disk. Different line types indicate Sample 1 (solid lines), Sample 2 (dashed lines) and Sample 2 (dotted lines). Right panels: Median ellipticity of the projected host halos as a function of the ellipticity of the projected disks. Different point types indicate Sample 1 (stars), Sample 2 (circles) and Sample 3 (triangles).

rounder projected halos for edge—on hosts disks and very slightly flatter projected halos for face—on host disks.

The reason that the median projected halo ellipticity is at best weakly dependent on the ellipticity of the host's projected disk is that the probability distributions of the halo ellipticities, $P(\epsilon_{\text{halo}})$, are only weakly dependent on ϵ_{disk} . We illustrate this in Figure 6 where we show $P(\epsilon_{\text{halo}})$ for the $\vec{J_c}$ hosts as a function of the ellipticities of the projected disks. Since $P(\epsilon_{\text{halo}})$ changes only mildly from panel to panel in Figure 6, it is clear that selecting host galaxies on the basis of highly-elliptical images does not preferentially select the very flattest halos, nor does it exclude the very roundest halos. This in mind, we expect the location angles of the satellites of hosts that are selected on the basis of the flatness of their images (as opposed to the flatness of their dark matter halos) will show much less anisotropy than we found in §3 above.

Like Figure 2 in the previous section, Figure 7 shows the differential and cumulative probability distributions for the location angles of the GIF satellites. Here, however, ϕ is measured with respect to the major axes of the hosts' projected circular disks rather than with respect to the major axes of the hosts' projected halos. This change in the definition of the symmetry axis that is used to measure the location angles of the satellites has a marked affect on the probability of a satellite having a given location angle, ϕ . In the case of the J_c hosts, the hosts' circular disks lie in the principle planes of the halos and the satellites clearly still prefer alignment with the major axes of the hosts. However, the degree of anisotropy is reduced from that in Figure 2 and here the median value of the location angle is $\phi_{\rm med} \sim 35^{\circ}$ (c.f. $\phi_{\rm med} \sim 29^{\circ}$ in the previous section). Aligning the angular momentum vectors of the hosts' disks with the net angular momentum vectors of the hosts' halos (i.e., the $\vec{J}_{\rm ang}$ hosts) results in the satellites having a rather weak preference for being aligned with the major axes of their hosts ($\phi_{\rm med} \sim 42^{\circ}$). When the angular momentum vectors of the hosts disks are aligned with the intermediate axes of the local large scale structure (i.e., the J_{lss} hosts) the distribution of satellite location angles becomes nearly isotropic ($\phi_{\rm med} \sim 44^{\circ}$). As expected from Figure 5, the misalignment of mass and light in these host galaxies, as well as the inclusion of halos that are round in projection, results in a reduction of the anisotropy that was found when the satellite location angles were measured relative to the projected major axes of markedly flattened host halos (i.e., §3). Finally, an extremely strong "Holmberg effect" is produced when the angular momentum vectors of the hosts' disks are aligned with the major axes of the halos' virial mass. That is, the satellites of the \vec{J}_a hosts show a strong preference for being clustered near the minor axes of the hosts, yielding a median location angle of $\phi_{\rm med} \sim 57^{\circ}$.

Because the selection of hosts based upon flattened images (i.e., $\epsilon_{\rm disk} > 0.2$) is not

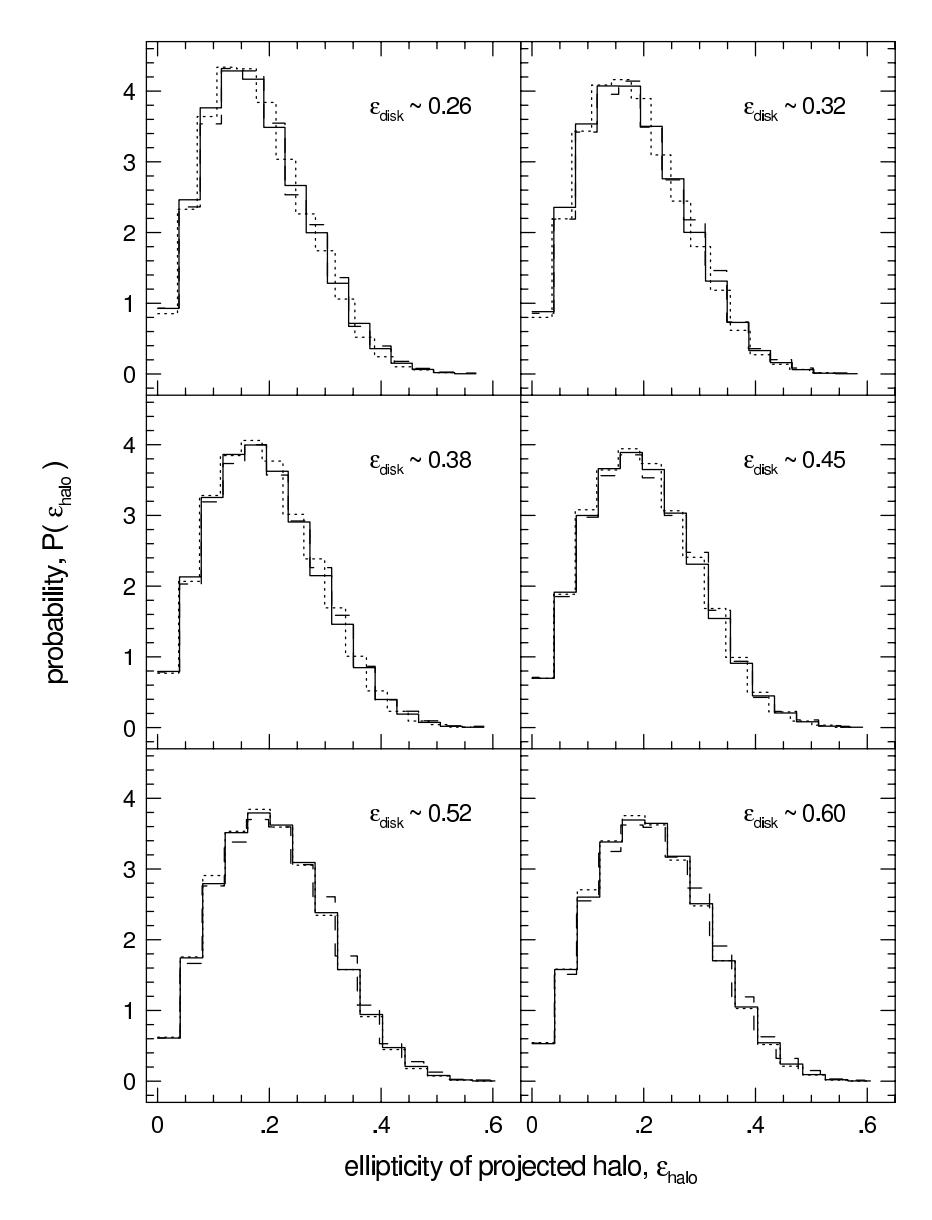


Fig. 6.— Probability distribution of the projected host halo ellipticity, $P(\epsilon_{\text{halo}})$, for $\vec{J_c}$ hosts with different projected disk ellipticities, ϵ_{disk} . Different line types show Sample 1 (solid lines), Sample 2 (dashed lines) and Sample 3 (dotted lines). Host halos are defined to be all particles within r_{200} .

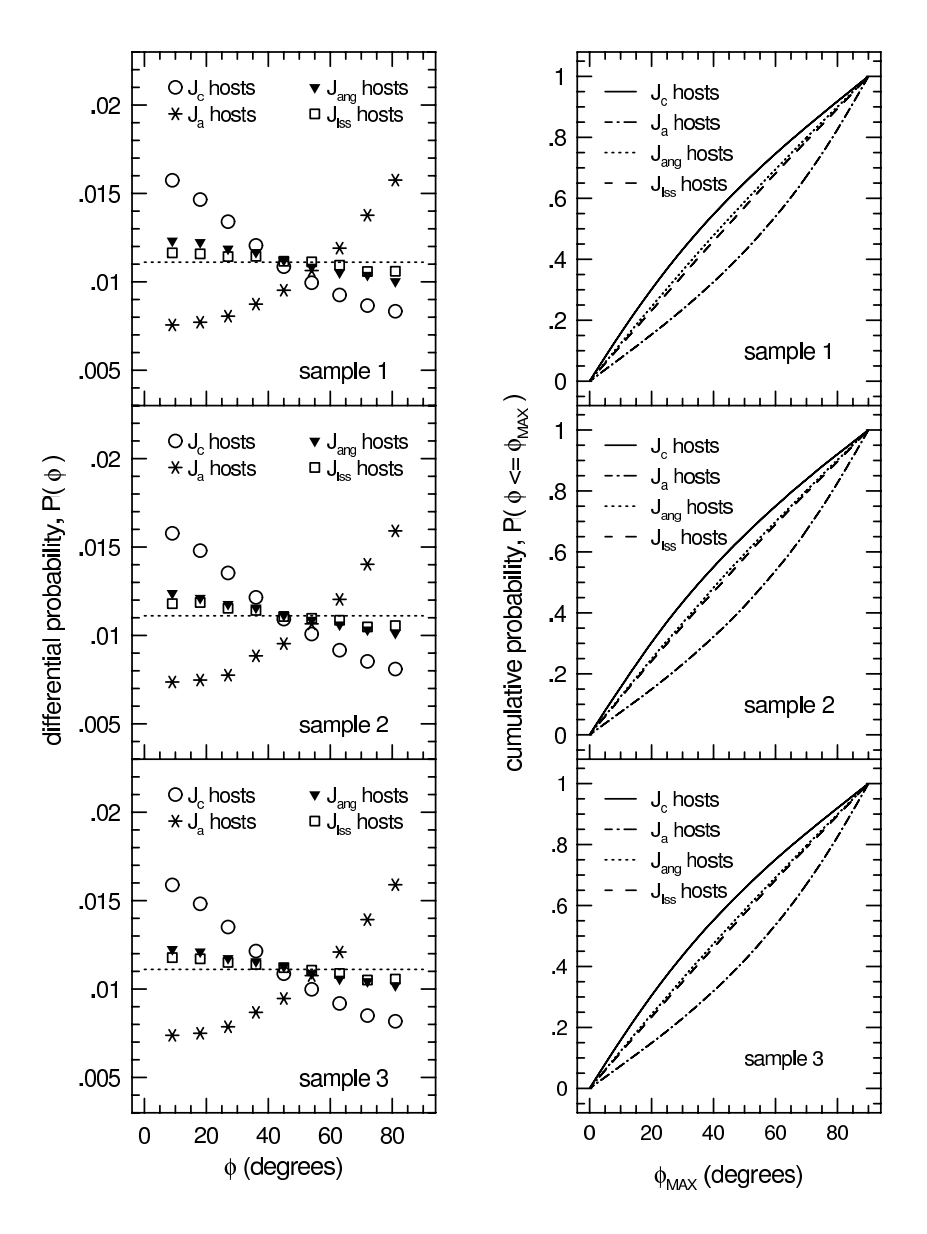


Fig. 7.— Probability distributions for the location angles of satellite galaxies, measured with respect to the major axes of the projected disks of their hosts. Hosts are required to have a projected ellipticity of $\epsilon_{\rm disk} > 0.2$. All satellites with $r_p < 500$ kpc are used. Left panels: Differential probability distributions. Different point types show results for the $\vec{J_c}$ hosts (open circles), $\vec{J_a}$ hosts (stars), $\vec{J_{\rm ang}}$ hosts (filled triangles), and $\vec{J_{\rm lss}}$ hosts (open squares). Right panels: Cumulative probability. Different line types show results for the $\vec{J_c}$ hosts (solid lines), $\vec{J_a}$ hosts (dash-dot lines), $\vec{J_{\rm ang}}$ hosts (dotted lines), and $\vec{J_{\rm lss}}$ hosts (dashed lines). In all panels the axis scales are identical to the corresponding panels in Figure 2 for comparison.

equivalent to selecting hosts on the basis of flattened halos (i.e., Figures 5 and 6), we expect that the degree of anisotropy shown by the satellite location angles in this section should, at best, be weakly dependent on the shape of the hosts' projected disks. This is shown by the left panels of Figure 8 in which the open points indicate the dependence of $\phi_{\rm med}$ on the ellipticity of the hosts' disks, $\epsilon_{\rm disk}$. Also shown for comparison in these panels is the dependence of $\phi_{\rm med}$ on $\epsilon_{\rm halo}$ from the top panel of Figure 3 (crosses). In the cases of the $\vec{J}_{\rm ang}$ and $\vec{J}_{\rm lss}$ hosts, the large offset in projected mass compared to projected light results in $\phi_{\rm med}$ for the satellites being essentially independent of the ellipticity of the hosts' images. In the cases of the \vec{J}_c and \vec{J}_a halos, the degree of anisotropy in the satellite location angles shows some dependence on $\epsilon_{\rm disk}$, but it is not nearly as pronounced as the dependence of the anisotropy on $\epsilon_{\rm halo}$. For both the \vec{J}_c and \vec{J}_a hosts, $\phi_{\rm med}$ for the edge—on hosts differs from $\phi_{\rm med}$ for the hosts with $\epsilon_{\rm disk} \sim 0.2$ by of order 10°, with the anisotropy being most pronounced for the edge—on hosts.

Finally, the dependence of $\phi_{\rm med}$ on projected radius, scaled by the virial radii of the hosts, is shown in the right panels of Figure 8. As was the case for satellite location angles measured relative to the major axis of the projected halo mass (i.e., bottom panel of Figure 3), the degree of anisotropy shown by the satellites of the \vec{J}_a and \vec{J}_c hosts is most pronounced for projected radii that are of order r_{200} . This dependence is not shown by the satellites of the $\vec{J}_{\rm ang}$ and $\vec{J}_{\rm lss}$ hosts, and in these cases $\phi_{\rm med}$ is largely independent of projected radius.

5. Discussion

We have used the Λ CDM GIF simulation to investigate the locations of satellite galaxies with respect to the major axes of their hosts and find that:

- 1. When the location angles of the satellites are measured with respect to the major axes of the projected host halos, the satellites exhibit an anisotropic distribution that traces the projected halo mass rather well.
- 2. If the mass and light of host galaxies are perfectly aligned in projection on the sky, then the sense of the anisotropy in the satellite location angles is the same as that shown by satellite galaxies in the SDSS (i.e., a preference for location nearby the major axis of the host's image). However, the magnitude of the anisotropy shown by the GIF satellites far exceeds that of the SDSS satellites since our analysis was restricted to the satellites of hosts with markedly flattened halos ($\epsilon_{\text{halo}} > 0.2$).
- 3. If all host galaxies are disk galaxies, there is only a weak correlation between the ellipticity of the projected disk, ϵ_{disk} , and the ellipticity of the projected halo, ϵ_{halo} . No

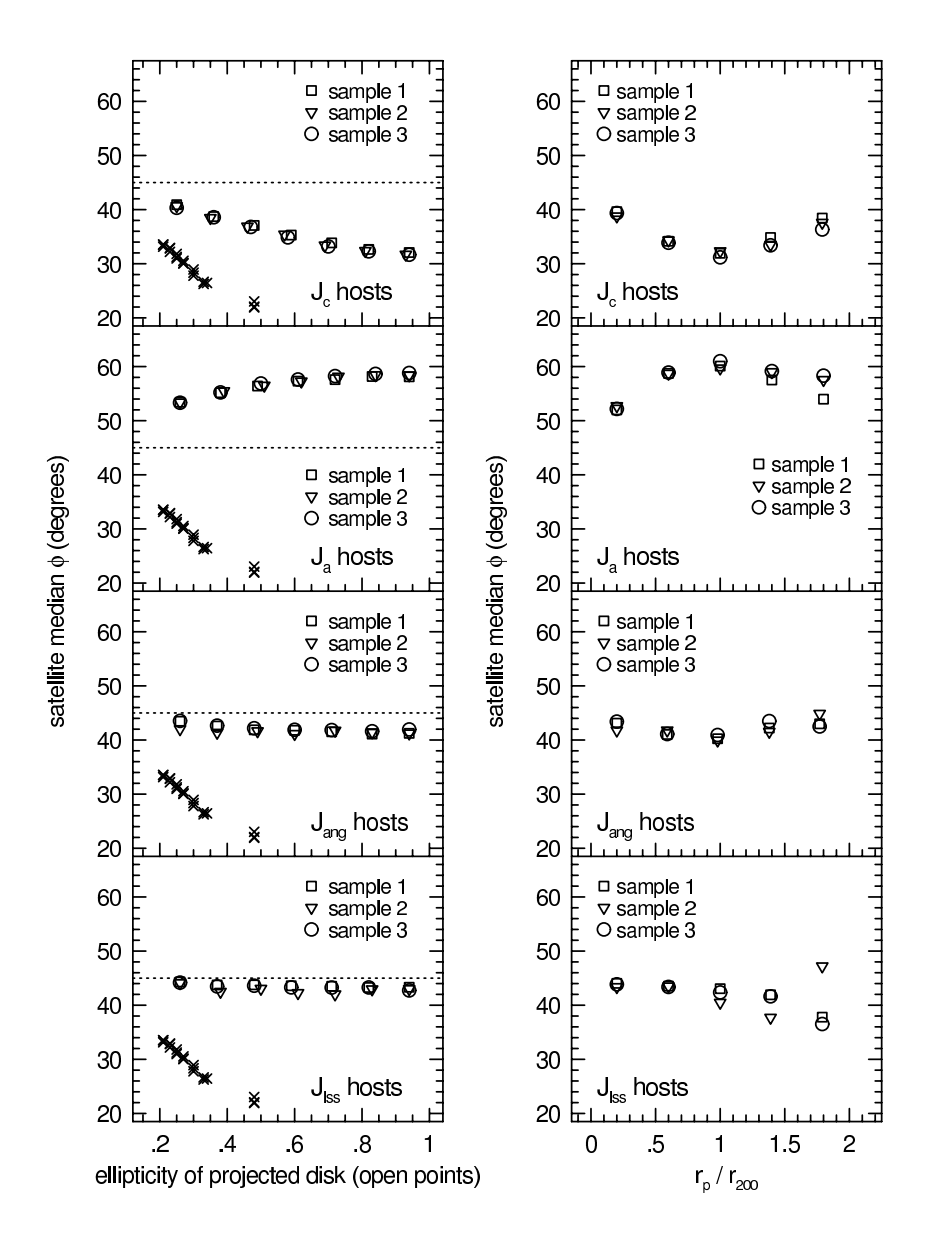


Fig. 8.— Left panels: Open points show the median satellite location angle, measured with respect to the major axis of the host galaxy's projected circular disk, as a function of the ellipticity of the host's disk. All satellites with $r_p < 500$ kpc have been used. For comparison, crosses show the median satellite location angle from the top panel of Figure 3 for all three samples as a function of the ellipticity of the projected host halo (i.e., here ϕ is measured with respect to the major axis of the projected host halo). Right panels: Median satellite location angle, measured with respect to the major axis of the host galaxy's projected circular disk, as a function of projected radius, r_p . Here r_p is measured in units of the host galaxy's virial radius, r_{200} .

matter how the disk is oriented within the halo, this alone reduces the anisotropy in the satellite location angles. This is because the satellites essentially trace the projected mass of the hosts' halos, and round halos are not rejected by simply requiring the image of the host to be rather elliptical (i.e., $\epsilon_{\text{disk}} > 0.2$).

4. If the location angles of the satellite galaxies are measured relative to the major axes of their host's projected disks, the resulting degree of anisotropy is strongly dependent upon the way in which the host disk is oriented inside its halo. A pronounced "Holmberg effect" (i.e., preference for location nearby the minor axes of the hosts) is obtained when the angular momentum vectors of the host disks are aligned with the major principle axes of the hosts' halos. A strong tendency for the satellites to be found nearby the major axes of the hosts (i.e., the type of anisotropy shown by the SDSS satellites) is obtained when the angular momentum vectors of the host disks are aligned with the minor principle axes of their halos. When the angular momentum vectors of the host disks are aligned with the net angular momentum vectors of their halos, the satellites have a tendency to be located nearby the major axes of their hosts, but the degree of anisotropy is considerably weaker than when the angular momentum vectors of the host disks are aligned with the minor axes of their halos. When the angular momentum vectors of the host disks are aligned with the intermediate principle axes of the local large scale structure, the location angles of the satellites become nearly isotropic.

We have shown that, provided mass and light are "reasonably" well–aligned in the host galaxies, Λ CDM naturally predicts that satellite galaxies should should be anisotropically distributed relative to the symmetry axes of their hosts and, specifically, the satellites should show a preference for being located nearby the major axes of their hosts. The sense of this anisotropy agrees well with the anisotropy shown by the satellites of host galaxies in the SDSS, but none of our simple prescriptions for defining the major axes of host galaxies in the GIF simulation precisely reproduces the magnitude of the anisotropy shown by the SDSS satellites ($\phi_{\rm med}^{\rm SDSS} \sim 40.5^{\circ}$). When we assume all host galaxies are disks and we align the disk angular momentum vectors with the minor principle axes of the host halos, the GIF satellites are distributed more anisotropically than are the SDSS satellites ($\phi_{\rm med}^{\rm GIF} \sim 35^{\circ}$). If, instead, we align the host disk angular momentum vectors with the net angular momentum vectors of their halos, the GIF satellites are distributed less anisotropically than are the SDSS satellites ($\phi_{\rm med}^{\rm GIF} \sim 42^{\circ}$). In addition, the anisotropy shown by the GIF satellites appears to persist to much larger projected radii than does the anisotropy shown by the SDSS satellites.

It is important to keep in mind that the GIF and SDSS hosts are by no means identical, if for no other reason than the resolution limit of the simulation restricts our analysis to

rather massive isolated host galaxies. In addition, since there are no images of the hosts in the simulation, we have used very simple arguments to precisely align the angular momentum vectors of the GIF hosts with their surrounding environments. In particular, we have had to use large physical scales (i.e., from r_{200} to 2.5 Mpc) to define the surrounding environment. However, work by Bailin et al. (2005) on the formation of disk galaxies in CDM universes suggests that the orientation of the disk tends to be aligned with only the inner halo, and that the relative orientation of the inner and outer halo are essentially uncorrelated. Further, at least some fraction of the SDSS hosts are elliptical galaxies and we have not allowed for this in our analysis. Finally, many of the host galaxies in the SDSS are obvious spirals and an exact determination of the "major axis" of such hosts is difficult because the light profiles are not smooth. This naturally introduces some level of error in the observational determination of the locations of satellite galaxies around their hosts, and serves to decrease the measured anisotropy compared to the true anisotropy that one would obtain if the host position angles were known to arbitrary accuracy.

There are two previous numerical studies of the locations of luminous satellite galaxies that are directly comparable to our work here. Both Libeskind et al. (2005) and Zentner et al. (2005) used semi-analytic galaxy formation to study the locations of luminous satellites (i.e., rather than extrapolating from a pure dark matter simulation). There are, however, a number of important differences between the Libeskind et al. (2005) and Zentner et al. (2005) investigations and the investigation presented here. First, both Libeskind et al. (2005) and Zentner et al. (2005) used simulations with much smaller volumes and much higher resolution in order to address the apparent planar clustering of the Milky Way's satellite galaxies. In their simulations Libeskind et al. (2005) and Zentner et al. (2005) were restricted to the study of only a small number of hosts (6 and 3, respectively), each of which had a large number of satellites, and the distribution of the satellites was computed independently for each host halo. Here we have used a large number of hosts with a wide range of masses and luminosities and, since most of our hosts have only a few satellites, our results for the distribution of the satellites is obtained by effectively "stacking" all of the host-satellite systems together. That is, Libeskind et al. (2005) and Zentner et al. (2005) investigated what Λ CDM predicts specifically for host galaxies that are like the Milky Way, while our study investigates what Λ CDM predicts for large redshift surveys in which one is limited to only a few satellites per host.

Neither Libeskind et al. (2005) nor Zentner et al. (2005) selected host–satellite systems in a way that mimics what is commonly done with large redshift surveys. Libeskind et al. (2005) combined semi–analytic galaxy formation with their N–body simulations and, so, there are truly luminous satellite galaxies (as opposed to simply "subhalos") present in the simulations. The satellites used by Libeskind et al. (2005) consist of the 11 most luminous

satellites of each host galaxy, in analogy with the Milky Way system. Zentner et al. (2005) use two techniques to select satellites: semi-analytic galaxy formation and an association of satellites with the most massive surviving subhalos. Both Libeskind et al. (2005) and Zentner et al. (2005) conclude that the satellite populations of their Milky Way systems are strongly flattened into thin, somewhat disk-like structures that are aligned with the longest principle axis of the dark matter halos of the host galaxies. They further conclude that, in the case of the Milky Way, the observed distribution of the satellites implies that the longest principle axis of the Milky Way's halo is oriented perpendicular to the disk. (It should be noted, however, that there are no actual luminous disks for the host galaxies in these simulations so neither study demonstrated directly that the disks of host galaxies are anti-aligned with the longest principle axes of the halos.)

Our work here agrees well with the sense of the anisotropy of the satellite locations found by Libeskind et al. (2005) and Zentner et al. (2005); the satellites are found in a flattened, rather than spherical, distribution and that distribution is aligned well with the longest principle axis of the halo of the host galaxy. In addition, we concur with their result that satellite galaxies should be located preferentially close to the minor axes of the images of their hosts if the host galaxy is a disk that has its angular momentum aligned with the major principle axis of its halo (i.e., the satellites of our $\vec{J_a}$ hosts). However, since there are typically only one or two GIF satellites per host galaxy, we cannot address the question as to whether the satellites of any one host galaxy are generally found to lie in an extremely flattened, nearly-planar structure. Like the results of Libeskind et al. (2005) and Zentner et al. (2005), however, our results for the anisotropic distribution of the GIF satellites certainly do seem to be a reflection of the fact that satellites are accreted preferentially along filaments.

Whether or not the locations of satellite galaxies in CDM universes agree with the locations of satellite galaxies in large redshift surveys remains an open question. Here we have shown that the sense of the observed anisotropy (a preference for clustering of satellites nearby the major axes of the images of host galaxies) is consistent with the sense of the anisotropy that one would expect in a CDM universe, under the assumption that the major axes of the images of host galaxies are at least modestly correlated with the major axes of their projected halos. A proper resolution to the discrepancies that we find between observation and theory awaits simulations that are of considerably higher resolution and which address the details of the orientations of the visible hosts with respect to their dark matter halos.

Acknowledgments

We grateful to Mario Abadi, Brad Gibson, and Julio Navarro for discussing their work with us in advance of its publication and to Simon White for helpful suggestions. We also thank the referee for truly constructive criticisms that improved the manuscript. Support under NSF contract AST-0406844 (IA, TGB) is gratefully acknowledged.

REFERENCES

Bailin, J., Kawata, D., Gibson, B., Steinmetz, M., Navarro, J. F., Brook, C. B., Gill, S. P. D., Ibata, R. A., Lewis, G. F. & Okamoto, T. 2005, submitted to ApJ

Brainerd, T. G. 2004, submitted to ApJ (astro-ph/0409381)

Brainerd, T. G. 2005, 628, L101

Guzik, J. & Seljak, U. 2002, MNRAS, 335, 311

Hoekstra, H., Yee, H. K. C. & Gladders, M. D. 2004, ApJ, 606, 67

Holmberg, E. 1969 Ark. Astron., 5, 305

Kauffmann, G., Colberg, J. M., Diaferio, A. & White, S. D. M. 1999, MNRAS, 303, 188

Kazantzidis, S., Kravtsov, A. V., Zentner, A. R., Allgood, B., Nagai, D. & Moore, B. 2004, ApJ, 611, L 2004

Keeton, C. R., Kochanek, C. S. & Falco, E. E. 1998, ApJ, 509, 561

Kleinheinrich, M., Schneider, P., Rix, H.-W., Erben, T., Wolf, C., Schirmer, M., Meisenheimer, K., Borch, A., Dye, s., Kovacs, Z., & Wisotzki, L. 2004, submitted to A& A (astro-ph/0412615)

Knebe A., Gill S.P.D., Gibson B.K., Lewis G.F., Ibata R.A., Dopita M.A. 2004, ApJ, 603, 7

Libeskind, N. I., Frenk, C. S., Cole, S., Helly, J. C., Jenkins, A., Navarro, J. F. & Power, C. 2005, MNRAS, 363, L146

Lynden-Bell, D. Obs., 102, 202

Majewski, S. R. 1994, ApJ, 431, L17

Moore, B., Ghigna, S. et al. 1999, ApJ, 524, L19

Navarro, J. F., Abadi, M. G. & Steinmetz, M. 2004, ApJ, 613, L41

Navarro, J. F., Frenk, C. S. & White, S. D. M. 1995, MNRAS, 275, 720

Navarro, J. F., Frenk, C. S. & White, S. D. M. 1996, ApJ, 462, 563

Navarro, J. F., Frenk, C. S. & White, S. D. M. 1997, ApJ, 490, 493

Norberg, P., Cole, S., Baugh, C. M., Frenk, C. S., Baldry, I., Bland-Hawthorn, J., Bridges, T., Cannon, R., Colless, M., et al. 2002, MNRAS, 336, 907

Prada, F., Vitvitska, M., Klypin, A., Holtzman, J. A., Schelgel, D. J., Grebel, E., Rix, H.-W., Brinkmann, J., McKay, T. A. & Csabai, I. 2003, ApJ, 598, 260

Sackett, P.D. 1999, in "Galaxy Dynamics", ASP Conf. Series 182, eds. D. R. Merritt, M. Valluri & J. A. Sellwood, 393

Sales, L. & Lambas, D. G. 2004, MNRAS, 348, 1236

Simien, F. & De Vaucouleurs, G., 1986, ApJ, 302, 564

Smith, J. A., et al. 2002, AJ, 123, 2121

Zaritsky, D., Smith, R., Frenk, C. & White, S. D. M., 1997, ApJ, 478, 39

Zentner, A. R., Kravtsov, A., Gnedin, O. Y. & Klypin, A. A. 2005, ApJ, 629, 219

This preprint was prepared with the AAS LATEX macros v5.2.